

Hybridization Phenomena in Nearly-Half-Filled f -Shell Electron Systems: Photoemission Study of EuNi_2P_2

S. Danzenbächer,¹ D. V. Vyalikh,¹ Yu. Kucherenko,^{1,2} A. Kade,¹ C. Laubschat,¹ N. Caroca-Canales,³ C. Krellner,³ C. Geibel,³ A. V. Fedorov,⁴ D. S. Dessau,⁵ R. Follath,⁶ W. Eberhardt,⁶ and S. L. Molodtsov¹

¹*Institut für Festkörperphysik, Technische Universität Dresden, D-01062 Dresden, Germany*

²*Institute for Metal Physics, National Academy of Sciences of Ukraine, UA-03142 Kiev, Ukraine*

³*Max-Planck-Institut für Chemische Physik fester Stoffe, Nöthnitzer Strasse 40, D-01187 Dresden, Germany*

⁴*Advanced Light Source, Lawrence Berkeley National Laboratory, Berkeley, California 94720, USA*

⁵*Department of Physics, University of Colorado, Boulder, Colorado 80309, USA*

⁶*BESSY GmbH, Albert-Einstein-Strasse 15, D-12489 Berlin, Germany*

(Received 9 July 2008; published 14 January 2009)

The mixed-valent compound EuNi_2P_2 was studied by photoemission. Observed splittings and dispersions of the Eu $4f^6$ final state close to energy crossings of the Eu $4f$ and Ni $3d$ states are explained in terms of hybridization by a momentum and energy dependence of the electron hopping matrix element. These data obtained for a system with more than one $4f$ electron (hole) show that dispersions and hybridization gaps related to Kondo and heavy-fermion behavior can be found in other rare-earth-metal compounds apart from Ce and Yb-based ones.

DOI: 10.1103/PhysRevLett.102.026403

PACS numbers: 71.27.+a, 71.20.Eh, 75.30.Mb, 79.60.-i

In the last few years considerable attention has been paid to studying quantum-critical phenomena in rare-earth-metal (RE) intermetallic compounds like transitions between magnetism, superconductivity, and heavy-fermion (HF) behavior as a function of external parameters including pressure or chemical composition [1]. The main driving force of these astonishing correlated phenomena are strongly localized $4f$ electrons, which interact with itinerant valence electrons delocalized throughout the crystal lattice. Upon increasing this interaction the ground state of the RE intermetallic compounds evolves from magnetic order established via spin polarization of conduction electrons (RKKY mechanism) to the Kondo state with screened magnetic moments (Kondo effect) and finally to the mixed-valent state [2]. A periodic arrangement of the Kondo impurities into the Kondo lattice may result in the thousand-fold increase of the electron effective mass compared to the mass of a free electron (m_0) [3], which is the landmark of the HF behavior.

This possibility to tune the magnetic state allows to study quantum-phase transitions in detail [4]. Especially their relations to unconventional superconductivity [5] are a central topic of current investigations, both for the relevance of our fundamental understanding of solid-state physics and for dedicated search for new high-temperature superconductors [6]. Unlike widely studied Ce and Yb systems, Eu-based intermetallic compounds are a rather unexplored field in this context. They are, however, of high interest for studies, since inherent differences to Ce- and Yb-based systems should allow to gain a better understanding of the mechanism and phenomena relevant at quantum-critical points [7].

The most direct experimental insight into this problem may be expected from angle-resolved photoemission (PE)

experiments that reflect the momentum (\mathbf{k}) resolved response of the electronic system to a single $4f$ excitation, while transport, specific heat, and magnetization measurements integrate over many different excitations and large areas in \mathbf{k} space. The PE approach was successfully used to investigate a variety of Ce- and Yb-based HF and Kondo systems [8–11].

In this contribution we present high-resolution angle-resolved PE data of the mixed-valent compound EuNi_2P_2 that are complemented with numerical studies. The study focuses on the behavior of the $4f^6$ final state close to the Fermi energy (E_F). This state exhibits on the one hand a characteristic 7F_J multiplet splitting as expected from an atomiclike state, on the other hand additional splittings and dispersions like a valence state. The data are properly reproduced within a calculation that describes the interaction between the $4f$ and valence-band (VB) states in the framework of a simplified periodic Anderson model (PAM) [9,10]. While the presence of $4f$ dispersions and hybridization gaps in other than Ce and Yb compounds have been discussed in the literature since long time [12] our experiments give for the first time direct evidence for such phenomena by photoemission.

EuNi_2P_2 is a mixed-valent compound, which maintains its valence 2.5 for $T \rightarrow 0$ indicating that the valence fluctuation rate is particularly large here [13]. In PE spectra such a scenario is reflected by coexistence of two final-state multiplets, a narrow $4f^6$ (7F_J) multiplet at E_F and a broad $4f^5$ multiplet between 6 and 12 eV binding energies (BEs) [14,15].

Single crystalline EuNi_2P_2 samples were grown from Sn flux in evacuated quartz tubes and crystallize in body-centered tetragonal ThCr_2Si_2 - (I-) type structure [16]

shown in Fig. 1(a). It is formed by stacks of elemental layers which serve as natural cleavage planes. Hence, clean surfaces were prepared by cleaving samples in the ultra-high vacuum (10^{-11} -Torr range) by means of ceramic or metallic top posts glued at the crystal surfaces. Prior to the PE experiments the samples were characterized by x-ray diffraction, magnetic susceptibility, resistivity and specific heat measurements, confirming the results reported in the literature [13,17].

Angle-resolved PE studies were carried out at the Berliner Elektronenspeicherring für Synchrotronstrahlung (BESSY, beam line UE112-lowE-PGMb) and at the Advanced Light Source (ALS, beam line BL12.0.1). At both beam lines we have used light linearly polarized in either vertical or horizontal plane. The spectra were acquired using a Scienta R4000 electron-energy analyzer (BESSY) and a Scienta 100 analyzer (ALS). During the measurements samples were kept at ~ 20 K. The overall energy and angular resolutions were 15 meV and 0.2° , respectively. In our BESSY experimental geometry the analyzer slits were oriented at 45° (54° at ALS) to the synchrotron beam parallel to the vertical polarization direction of the incoming light [Fig. 1(b)]. Various photon energies in the range from $h\nu = 34$ eV to 55 eV were used to follow k_z dependent variations of the electronic structure. All selected photon energies provide high cross sections to monitor simultaneously PE contributions of the $4f$ and VBs of EuNi_2P_2 .

The electronic structure calculations were performed by means of the linear muffin-tin orbital (LMTO) method [18]. Because of the well-known failures of LDA-based approaches in description of the localized $4f$ states, the Eu $4f$ s were considered as quasicore states. Calculated LMTO band structure was then used to describe the effect of interaction on each spectral term of the Eu $4f$ multiplet by switching on the hybridization between the $4f$ and the VB states.

Strength of interaction with $4f$ states depends very much on symmetry and partial f character of the valence bands [9–11] that vary across the Brillouin zone (BZ). Particu-

larly strong interaction between individual terms of the 7F_J multiplet and a VB was experimentally found close to the **a** point of the surface BZ lettered in Fig. 1(c). The respective VB is formed mainly by Ni $3d$ states and is discussed below in detail.

Figure 2(a) shows a PE cut measured with vertical light polarization ($h\nu = 55$ eV) along the **b-a-b** direction ($\alpha = 6^\circ$) as indicated in Fig. 1(c). In this gray-scale plot the Eu $4f^6$ multiplet is seen in form of horizontal light stripes in the BE region from E_F down to 0.8 eV as a function of the emission angle β . It is superimposed by mainly Ni $3d$ -derived VBs crossing the multiplet terms at different **k** points. These “as measured” data reflect clearly the $4f$ –VB interaction within the area marked by the dashed circle. Surprisingly, a similar interaction effect is not seen

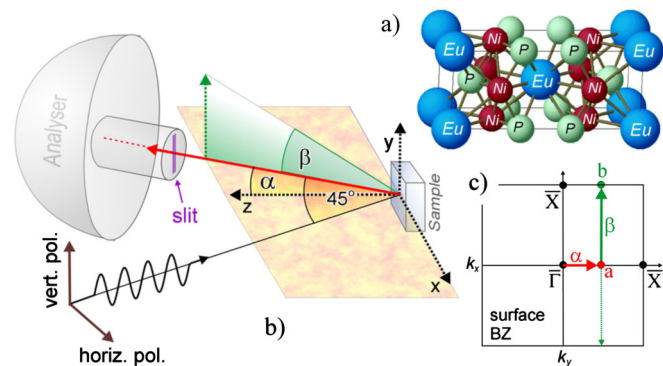


FIG. 1 (color online). (a) Crystal structure of EuNi_2P_2 , (b) experimental geometry and (c) surface BZ. Point **a** is located at 0.38 \AA^{-1} from $\bar{\Gamma}$ ($\alpha = 6^\circ$ at $h\nu = 55$ eV).

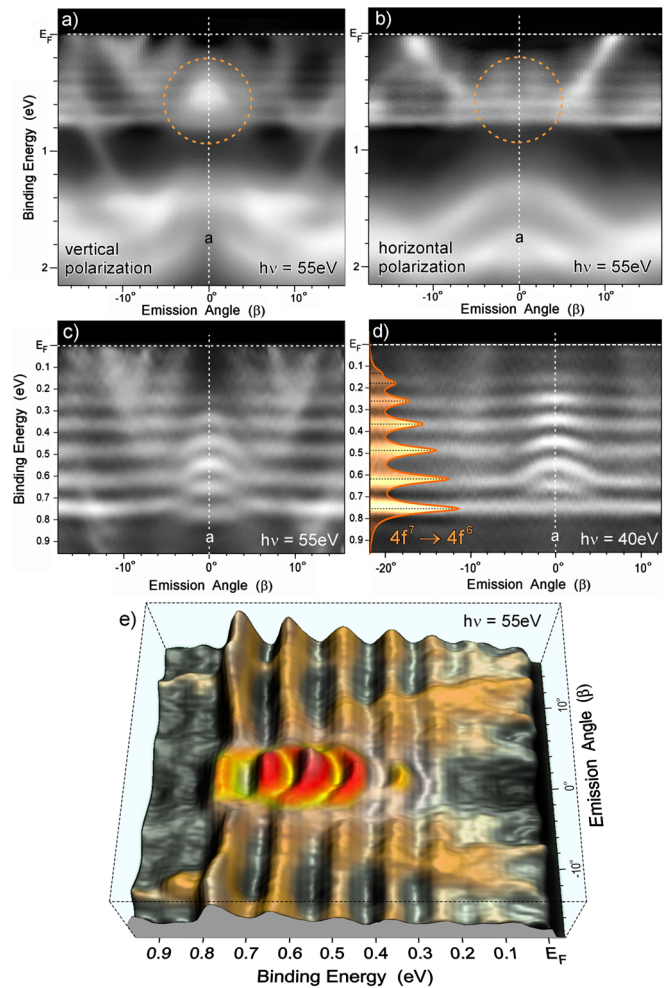


FIG. 2 (color online). PE cuts taken along the **b-a-b** direction with $h\nu = 55$ eV, vertical (a) and horizontal (b) linear light polarization. Light areas correspond to high PE intensity. Point **a** of the surface BZ corresponds to the emission angle $\beta = 0^\circ$. (c) Blow up of the (a) data taken with vertical polarization. (d) PE cut taken with $h\nu = 40$ eV, vertical light polarization. The calculated Eu $4f^6$ multiplet [14] broadened in accordance with the experimental data is shown at the energy axis. (e) Three-dimensional (3D) plot of the data depicted in (c).

in the data taken with horizontal light polarization [see Fig. 2(b)].

To explain this polarization dependence we consider the dipole matrix elements for the given geometry of the experiment. For the vertical polarization the transitions from the $3d_{yz}$ states contribute by $\sim 95\%$ to the Ni intensity. At the Eu sites these states can build the linear combinations with the point symmetry E_u in the form $f_{(5z^2-1)y}$ [denoted below as $f(E_u)$] and hybridize with the Eu $4f$ orbitals of the same symmetry ($m = \pm 1$). Particularly, these f orbitals dominate the Eu emission for the vertical polarization (94%). For the horizontal polarization the Eu emission is determined up to 86% by transitions from the $4f_{(5z^2-3)z}$ orbitals ($m = 0$) that are prohibited to interact with the VBs.

In the following we analyze the high-resolution experimental results taken with vertically polarized light [Fig. 2(c)]. The individual peaks of the $4f^6$ multiplet are densely packed over the 0.7 eV stretch. They partly overlap each other in energy. Therefore, to emphasize the observed hybridization phenomena, individual PE spectra contributing to the gray-scale plot shown in Fig. 2(c) were deconvoluted with a Gaussian (100 meV, full width at half maximum) accounting for the finite life time of the PE final state. One clearly recognizes that individual peaks of the Eu $4f^6$ multiplet do not run horizontally along **b-a-b**. At the emission angle $\beta = 0^\circ$ [corresponds to **a**, Fig. 1(c)] the energy positions of the peaks are no longer identical to the calculated energies of the atomic multiplet [see Fig. 2(d)]. Around **a**, the crossing of the $4f$ s with a holelike VB does not lead to a simple superposition of Eu $4f$ - and Ni $3d$ -derived intensities as observed in other places of the BZ. Instead, splittings and dispersions of the individual $4f^6$ components are monitored. This is an unambiguous manifestation of the hybridization between the Eu $4f$ and VB states.

Our data evidence that only certain VB states with specific symmetry can hybridize with the localized $4f$ states in selected regions of the BZ. The strength of hybridization affecting individual terms of the $4f$ multiplet can be tuned by changing the energy position of the responsible holelike VB throughout the BZ as shown in Fig. 2(d). Here, the data taken with $h\nu = 40$ eV at \mathbf{k}_z others than in Fig. 2(c) are presented. In the corresponding region of the BZ the holelike Ni $3d$ originating band is shifted upwards and an interaction pattern different to Fig. 2(c) is acquired. Similar to the magnitude of splittings and dispersions, the intensity behavior reflects the strength of the hybridization phenomena [Fig. 2(e)].

This hybridization could only be observed in the restricted \mathbf{k} region where the VB with high $f(E_u)$ contribution overlaps in energy the Eu $4f$ states (Fig. 2). The energy position of the holelike band with the high $f(E_u)$ character depends strongly on \mathbf{k}_z that is not well defined in PE. In the present case we expect, however, that the top of this band lies close to the energies where the splitting of the

Eu $4f$ states is observed [Fig. 3(a)]. For $h\nu = 55$ eV this is achieved if the \mathbf{k}_z point is chosen on the halfway between Γ and the upper edge of the bulk BZ ($\mathbf{k}_z = 0.17 \text{ \AA}^{-1}$). This choice is also supported by a \mathbf{k}_z estimation within the free-electron model for PE.

When going from $\bar{\Gamma}$ to \bar{X} the splittings and dispersions are only seen close to the **a** point (0.48 of the $\bar{\Gamma}$ - \bar{X} distance) that corresponds to the measurements performed at the polar angle $\alpha = 6^\circ$. Along the **b-a-b** direction, the highest $f(E_u)$ character of the band is calculated at the **a** point as well [Fig. 3(b)]. On both sides of **a**, the $f(E_u)$ character decreases and the VBs disperse towards higher BE, so that hybridization is no longer possible.

For the calculation of the $4f$ emission the interaction with the VB is taken into account by means of the hybridization model developed in Refs. [9,10]. The nondiagonal hybridization matrix element is given as

$$V_{\mathbf{k}}(E) = \Delta c_f(E, \mathbf{k}), \quad (1)$$

where Δ is the constant adjustable hybridization parameter and $c_f(E, \mathbf{k})$ are the calculated f -projected local expansion coefficients of the Bloch functions around the Eu site. The hybridization effect on the Eu $4f$ states decreases with increasing energy separation between the interacting elec-

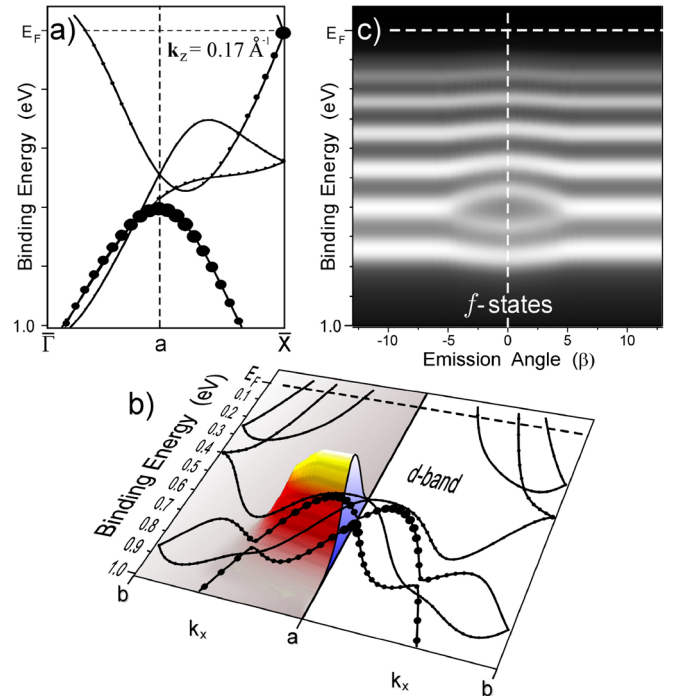


FIG. 3 (color online). (a) Band structure along $\bar{\Gamma}$ - \bar{X} projected on (001) surface BZ. Band character is indicated by dots with sizes proportional to the $f(E_u)$ contribution. (b) Band structure along **b-a-b** together with the assumed \mathbf{k} distribution of the VB $f(E_u)$ character (3D representation) taken as input parameter for the PE spectra simulation (see text). (c) Simulated f character PE spectra of EuNi_2P_2 . The obtained shift (splitting) of the $4f$ signals scales with hybridization strength $V_{\mathbf{k}}(E)$ calculated at each particular (\mathbf{k}, E) point.

tronic states. The calculations were performed for each Eu $4f$ multiplet component, then all obtained spectra were superimposed. The calculated spectral signals were broadened to simulate life-time effects and a finite instrumental resolution.

Similar to Ref. [10] we performed model calculations with a simplified VB structure in order to convincingly pick up the most important experimental features. The bunch of the VBs in the vicinity of \mathbf{a} is approximated by a \mathbf{k} -resolved $f(E_u)$ character density of states (DOS) with a holelike parabolic dispersion [Fig. 3(b)]. The degree of the $f(E_u)$ character of the DOS is accounted for by \mathbf{k} -slice areas in the 3D plot (see, e.g., slice through the \mathbf{a} point). It is correlated with the \mathbf{k} -resolved $f(E_u)$ character of the whole calculated VB envelope. The use of the model band structure is justified by small energy splittings between individual bands (~ 100 meV) as well as by uncertainties in \mathbf{k} space caused by nonconservation of \mathbf{k}_z in PE experiments. The energies and relative intensities of the non-perturbed final state Eu $4f^6$ -multiplet components shown in Fig. 2(d) were taken from Ref. [14].

The calculated 55-eV f spectra for emission angles $|\beta| > 6^\circ$ are only slightly affected by hybridization due to the weak $f(E_u)$ character of the bands in the corresponding region of the BZ. These spectra reveal six peaks that can be assigned to the terms from 7F_6 (most intense) to 7F_1 . The ground-state 7F_0 component is characterized by very low intensity and is not clearly resolved.

Comparing the above behavior with the one obtained for $\beta = 0^\circ$, where strong hybridization is expected, we see that the 7F_1 and 7F_2 components remain basically unchanged, 7F_3 and 7F_4 are shifted upwards and 7F_6 downwards, respectively, in accordance with the relative position and energy separation to the holelike VB allowed for hybridization with the Eu $4f$ states. The 7F_5 component is split into two features. The energy splitting at the \mathbf{a} point was used to estimate the hybridization parameter Δ . The obtained value $\Delta = 0.35$ eV matches the expected decrease of the hybridization parameter from Ce ($\Delta \sim 0.9$ eV) [9] to Yb ($\Delta \sim 0.2$ eV) [10] systems. When going from $\beta = 0^\circ$ towards $|\beta| \simeq 6^\circ$ the splitting becomes smaller giving rise to PE dispersion of the Eu $4f$ states. The simulated spectra are in good agreement with the experimental data shown in Figs. 2(a), 2(c), and 2(e).

Certainly, the presented theoretical consideration gives only a semiquantitative explanation of the observed phenomena. To the best of our knowledge, however, more rigorous models for the description of the many-body interactions of a $4f$ multiplet with VBs are not available. We show that our simplified approach with only one adjustable parameter Δ can be applied to understand the \mathbf{k} and energy dependent interactions in systems with more than one $4f$ electron (hole). To describe the phenomena we start from an atomiclike 7F_j multiplet and merge into the $4f$ dispersion scenario.

The obtained dualistic behavior of the $4f$ states shows that the quantum-critical phenomena related to the heavy-

fermion or Kondo behavior are expected in other RE compounds apart from Ce and Yb-based ones. With effective masses between 20 and $50m_0$, EuNi_2P_2 is still not a HF compound. The reason becomes obvious from the present data: In contrast to the high-BE lying multiplet components, the 7F_0 term that corresponds to the trivalent ground state of the system may only be weakly affected by hybridization. The reason is that nowhere in the BZ the holelike Ni $3d$ -derived band, which is responsible for the coupling, does approach E_F sufficiently [Figs. 2(c) and 2(d)]. In order to convert the system into a HF compound, the Fermi energy must be lowered with respect to the d bands. This might be achieved by substitution of Ni by earlier transition elements or P by more electronegative atoms.

This work was funded by the DFG, SFB 463, projects TP B4, B14 and B16, the Science and Technology Center in Ukraine (STCU), project 4930. The experiments at the ALS were supported by the DFG, project 444 USA 111/9/06, the Director, Office of Science, Office of Basic Energy Sciences of the U.S. Department of Energy under Contracts No. DE-AC02-05CH11231, DE-FG02-03ER46066, US NSF DMR 0706657.

-
- [1] P. Coleman and A. J. Schofield, *Nature (London)* **433**, 226 (2005); N. D. Mathur *et al.*, *Nature (London)* **394**, 39 (1998); S. S. Saxena *et al.*, *Nature (London)* **406**, 587 (2000); O. Stockert *et al.*, *Phys. Rev. Lett.* **92**, 136401 (2004).
 - [2] S. Doniach, *Physica (Amsterdam)* **91B+C**, 231 (1977).
 - [3] G. R. Stewart, *Rev. Mod. Phys.* **73**, 797 (2001); **78**, 743 (2006).
 - [4] P. Gegenwart *et al.*, *Nature Phys.* **4**, 186 (2008).
 - [5] D. M. Broun, *Nature Phys.* **4**, 170 (2008).
 - [6] P. C. Canfield, *Nature Phys.* **4**, 167 (2008).
 - [7] Z. Hossain *et al.*, *Phys. Rev. B* **69**, 014422 (2004).
 - [8] A. B. Andrews *et al.*, *Phys. Rev. B* **51**, 3277 (1995); **53**, 3317 (1996); H. Kumigashira *et al.*, *ibid.* **55**, R3355 (1997); A. J. Arko *et al.*, *ibid.* **56**, R7041 (1997); M. Garnier *et al.*, *ibid.* **56**, R11 399 (1997); J. Boysen *et al.*, *J. Alloys Compd.* **275–277**, 493 (1998).
 - [9] S. Danzenbächer *et al.*, *Phys. Rev. B* **72**, 033104 (2005); D. V. Vyalikh *et al.*, *Phys. Rev. Lett.* **96**, 026404 (2006); Yu. S. Dedkov *et al.*, *Phys. Rev. B* **76**, 073104 (2007).
 - [10] S. Danzenbächer *et al.*, *Phys. Rev. Lett.* **96**, 106402 (2006); S. Danzenbächer *et al.*, *Phys. Rev. B* **75**, 045109 (2007); S. L. Molodtsov *et al.*, *J. Magn. Magn. Mater.* **310**, 443 (2007).
 - [11] D. V. Vyalikh *et al.*, *Phys. Rev. Lett.* **100**, 056402 (2008).
 - [12] D. B. McWhan *et al.*, *Phys. Rev. B* **47**, 8630 (1993); T. Kasuya, *Europhys. Lett.* **26**, 277 (1994); P. A. Alekseev *et al.*, *J. Phys. Condens. Matter* **7**, 289 (1995); A. Barla *et al.*, *Phys. Rev. Lett.* **94**, 166401 (2005).
 - [13] R. Nagarajan *et al.*, *Phys. Rev. B* **32**, 2846 (1985).
 - [14] F. Gerken, *J. Phys. F* **13**, 703 (1983).
 - [15] G. Kaindl *et al.*, *Phys. Rev. B* **51**, 7920 (1995).
 - [16] H. F. Braun *et al.*, *Phys. Rev. B* **28**, 1389 (1983).
 - [17] R. A. Fisher *et al.*, *Phys. Rev. B* **52**, 13 519 (1995).
 - [18] O. K. Andersen, *Phys. Rev. B* **12**, 3060 (1975).